

A full 3D model of fluid flow and heat transfer in an E.B. heated liquid metal bath

A. Matveichev, A. Jardy, J.P. Bellot

Institut Jean Lamour - UMR 7198 CNRS/Université de Lorraine,
Laboratory of Excellence DAMAS, CS 50840, 54011 Nancy Cedex, France

E-mail: alain.jardy@univ-lorraine.fr

Abstract. In order to study the dissolution of exogeneous inclusions in the liquid metal during processing of titanium alloys, a series of dipping experiments has been performed in an Electron Beam Melting laboratory furnace. Precise determination of the dissolution kinetics requires knowing and mastering the exact thermohydrodynamic behavior of the melt pool, which implies full 3D modeling of the process. To achieve this goal, one needs to describe momentum and heat transfer, phase change, as well as the development of flow turbulence in the liquid. EB power input, thermal radiation, heat loss through the cooling circuit, surface tension effects (i.e. Marangoni-induced flow) must also be addressed in the model. Therefore a new solver dealing with all these phenomena was implemented within OpenFOAM platform. Numerical results were compared with experimental data from actual Ti melting, showing a pretty good agreement. In the second stage, the immersion of a refractory sample rod in the liquid pool was simulated. Results of the simulations showed that the introduction of the sample slightly disturbs the flow field inside the bath. The amount of such disturbance depends on the exact location of the dipping.

1. Introduction

The aim of this paper is to present recent development in IJL Nancy of a full 3D modeling of coupled fluid flow and heat transfer during the processing of liquid metal, and its implementation within the open source platform OpenFOAM. The model has been applied to the numerical modelling of Electron Beam heating and melting of a titanium alloy. A Ti button, placed in a water-cooled hemispherical copper crucible, is heated by an electron beam which moves very rapidly to repeat a given pattern of energy input. The flux density created by the beam leads to the melting of the metal and subsequent formation of a liquid bath.

Previously, an experimental study was performed to investigate the kinetics of dissolution of refractory metals such as W or Mo in liquid titanium alloys [1], in order to assess the possibility of HDI removal during Ti processing. This had been done by dissolving cylindrical rods dipped in molten titanium for controlled periods of time. A schematic representation of such experiment is given on Fig. 1.

Kinetics of the dissolution strongly depends on the liquid bath agitation and temperature, hence the necessity of a precise knowledge of the local temperature and velocity fields at the rod dipping



position. Since experimental measurement of these quantities is very difficult, it appeared that numerical simulation of the thermohydrodynamic behavior of the liquid bath was the best approach.

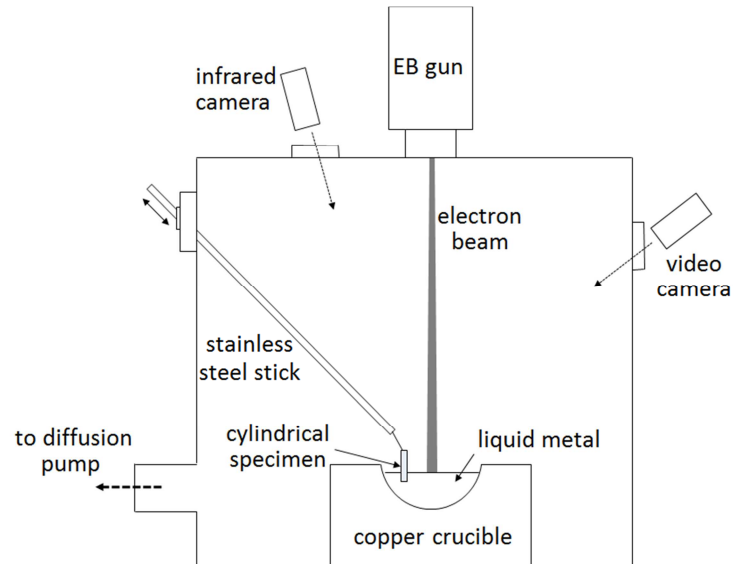


Figure 1. Scheme of a typical dipping experiment in the laboratory-scale 100 kW EB furnace at IJL Nancy.

2. Principle of the numerical model

The mathematical model accounts for various features that are responsible for the behavior of the metallic bath. Intense surface heating creates a Marangoni driven flow that, along with buoyancy effects, influences heat transfer and the steady-state liquid pool shape. Also, high surface velocities lead to the development of flow turbulence. Due to significant surface temperature, the radiative heat transfer is high and must be accounted for, as well as the heat loss through the crucible cooling circuit. The latter depends on the quality of the contact between the button and crucible. Therefore, the major physical phenomena which are simulated are listed in Table 1.

Table 1. The major physical phenomena considered in the model.

Heat transfer

- Heat transfer within the Ti sample by convection and conduction,
- Heat input by the electron beam,
- Radiation at the top surface,
- Phase change,
- Heat extraction by the cooling water circuit.

Momentum transfer

- Buoyancy caused by volumetric temperature gradients, and surface tension effects (Marangoni flow) related to surface temperature gradient,
- Turbulence development,
- Interaction between the solid and liquid within the mushy zone.

Space limitations do not allow us to give details of the constitutive equations used in the mathematical model, nor of their boundary conditions. Basically, they are similar to the ones used in classical CFD axisymmetrical models developed at IJL Nancy, such as the SOLAR and SOLECS codes used for simulating the Vacuum Arc Remelting and ElectroSlag Refining operations [2–5]. Certain specific features of the model are reported below, along with simplifying assumptions.

Typical timescale of the process is several minutes, much longer than the beam dwell time (a few milliseconds), so the energy input can be considered as uniformly distributed over the pattern, neglecting the actual motion of the beam. Assuming a constant back-scattering coefficient ξ , the incoming flux density φ_{EB} takes the following form:

$$\varphi_{EB} = (1 - \xi) \frac{W_{EB}}{A_{pat.}}$$

where W_{EB} is the total beam power and $A_{pat.}$ is the area covered by the beam pattern. Also, the deformation of the top free surface is neglected. Therefore, the shear stress τ caused by the tangential variation in surface tension with the temperature is expressed as:

$$\tau = \frac{\partial \gamma}{\partial T} \left(\vec{\nabla} T - \vec{n} (\vec{\nabla} T \cdot \vec{n}) \right)$$

where γ is the surface tension of liquid Ti alloy.

Velocity is set to zero at the metal/crucible interface (no slip). At this interface, heat transfer is calculated using the following equation:

$$\varphi_{cool} = \zeta(z) h_{cool} (T - T_w)$$

in which φ_{cool} is the heat loss, h_{cool} is a heat transfer coefficient that accounts for conduction in the crucible and copper-water interaction, and T_w is the temperature of the cooling water. Parameter $\zeta(z)$ was introduced to describe the quality of the contact between the metal and crucible. Basically, a better contact is obtained near the top of the button, while the cooling of the metal is liable to cause shrinkage near the bottom.

The set of coupled partial differential equations, which constitute the model, were solved numerically with a hybrid PISO-SIMPLE [6,7] algorithm. Time discretization was based on an implicit Euler scheme, while either the first-order upwind or the second-order van Leer scheme [8] was used for the discretization of convective terms. Laplacian (i.e. diffusive) terms were treated with a linear 2nd order scheme. The finite volume matrix was solved using preconditioned conjugate/bi-conjugate gradient methods [9,10].

Before advancing to the new time step, one needs to ensure full convergence of the solution. Following [11], residuals of the temperature, velocity, and pressure were checked, and the whole system was iterated until values between 10^{-2} and 10^{-6} were reached.

Asymmetric EB pattern requires a full 3D modeling. The solver was implemented within the OpenFOAM [12] framework so it is fully 3D, parallel and easily extensible with new physical models. The total number of cells was typically 500,000, while the time step for the calculations was initially set equal to 10^{-3} s and then controlled by a CFL condition. A weak parallelization (between 32 and 48 calculation nodes) was employed. The computational time required to obtain the results presented in next section was around 10 hrs.

3. Computed thermohydrodynamic behavior of the Ti button

In this section, typical results of the 3D model are presented, when applied to the case of Ti melting in the EB furnace. In order to validate the model, some simulation results are compared with experimental data on actual melting of a titanium button in our facility. Total beam power was 16 kW and the back-scattering coefficient was estimated at 0.3.

In the experiment, the 1.25 kg button was preheated with a circular beam pattern for the first 10 minutes, after which the beam was switched to a more complex 3D pattern and the button heated during another 20 minutes. The 3D beam pattern design consisted of one horizontal rectangle, two vertical rectangles and an arc, as shown on Fig. 2 (left). Such a horseshoe pattern was used as it allows to dip a refractory sample in a deep liquid pool at a location which does not directly interacts with the beam.

The actual pattern was reconstructed from successive frames extracted from a high-speed video of the process. The horseshoe shape is clearly visible on Fig. 2 (right), which shows that the center of the top arc was displaced 7 mm to the east and 3 mm to the north from the center of the button top surface. Vertical rectangles of the pattern were 2.1×3.5 cm in size, while the horizontal rectangle was 6.2×1.4 cm.

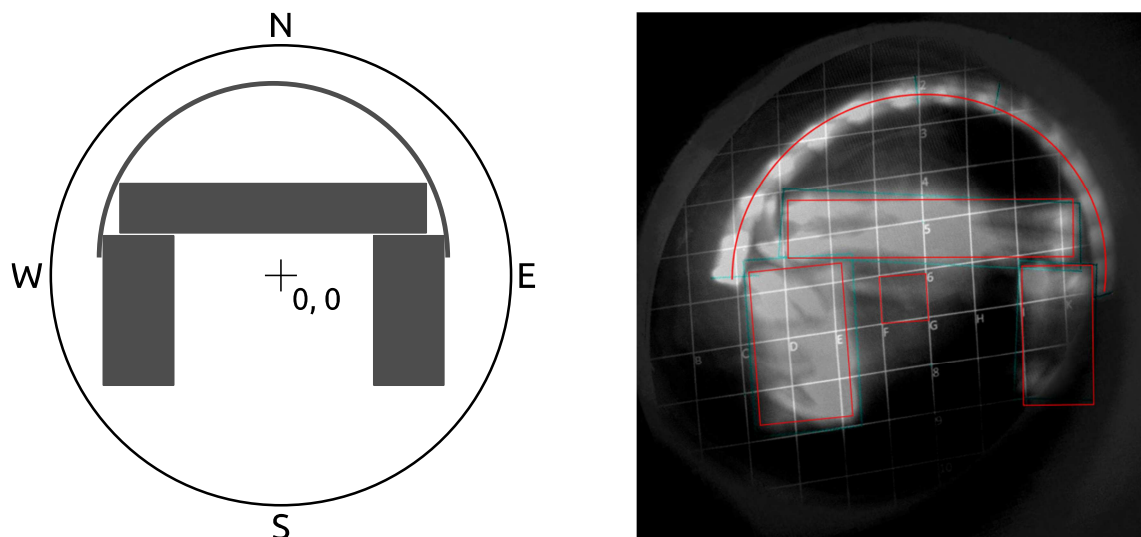


Figure 2. (left) design of the horseshoe beam pattern used during the last 20 minutes, (right) reconstruction of the actual pattern from high-speed films.

At $t = 0$, the solid metal is supposed to be at the room temperature. Figs 3 and 4 report the computed evolution of the liquid volume and the heating (by the beam) and cooling (radiation and contact) powers. Discontinuities at $t = 600$ s correspond to the abrupt change in the beam pattern, from circular to horseshoe. From these figures, it appears clearly that a steady state was fully reached after 30 minutes.

During the experiment, copper was introduced after 30 minutes into the liquid pool to mark its shape. The EB power was switched off and the button cooled rapidly. After full solidification and cooling, the button was cut every 5 mm in N-S and E-W directions (see Fig. 2 left) for reconstruction of the 3D liquid pool profile. The cutting scheme is shown on Fig. 5.

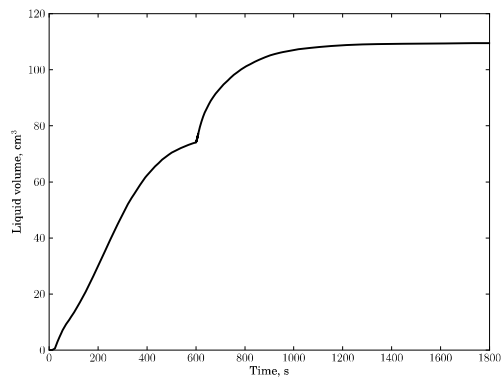


Figure 3. Computed evolution of the liquid volume

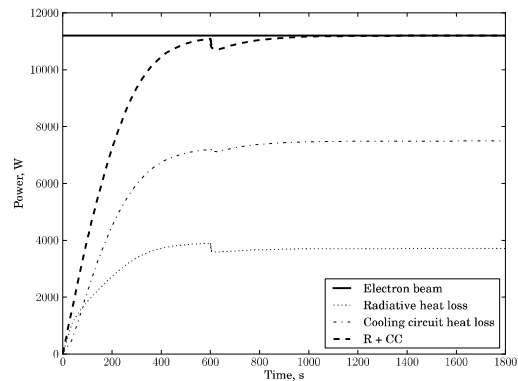


Figure 4. Computed evolution of the heating and cooling powers

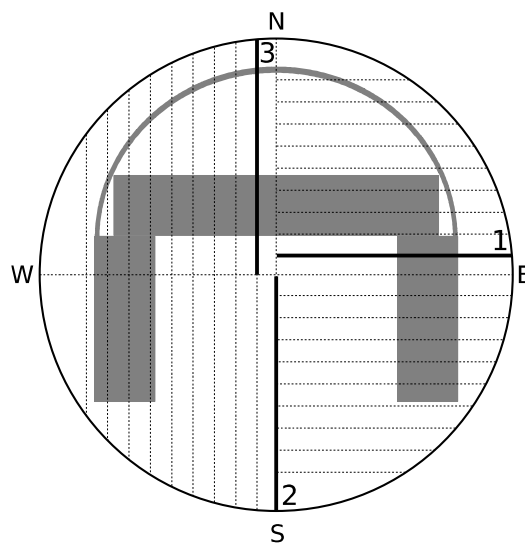


Figure 5. Cutting scheme of the solidified button. Bold numbered lines correspond to the the macrographs used to compare the observed profile shape with the simulation results

As shown on Fig. 5, three macrographs have been extracted for the sake of comparison between the computed and observed pool shape. These comparisons are the object of Figs 6 to 8.

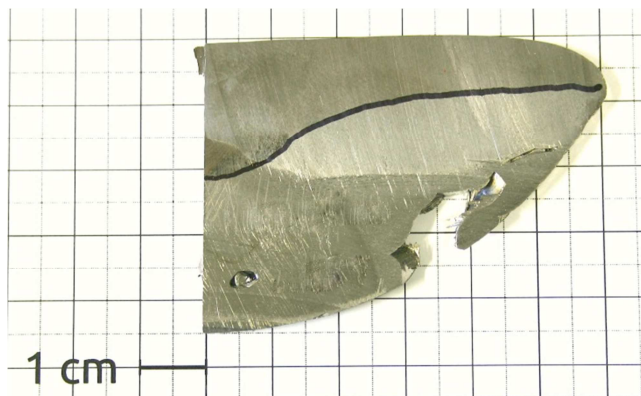
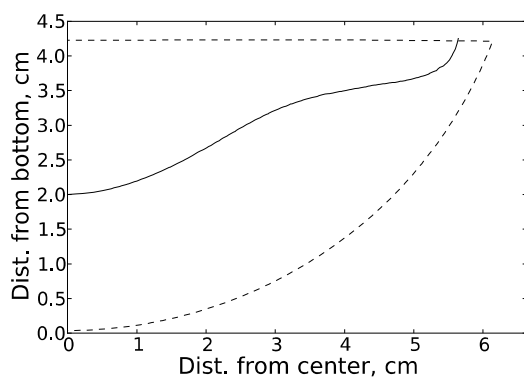


Figure 6. Melt pool profile intersection with plane 1 – (left) computed (right) observed

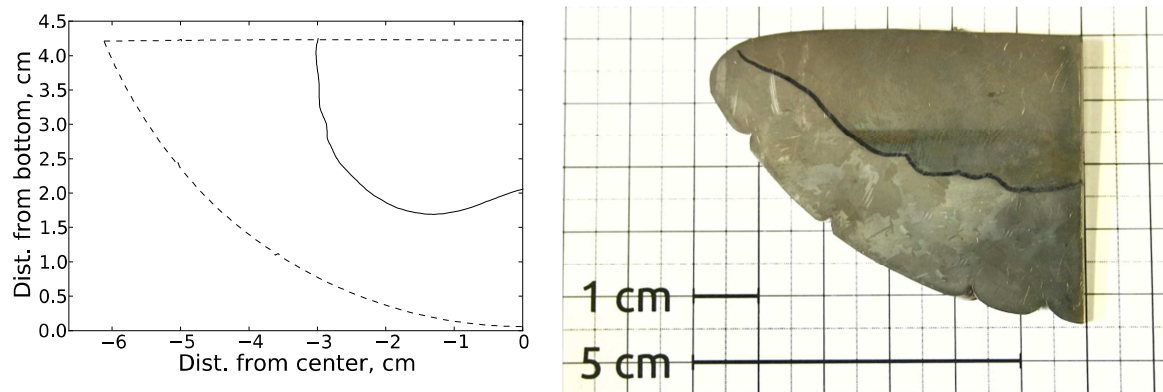


Figure 7. Melt pool profile intersection with plane 2 – (left) computed (right) observed

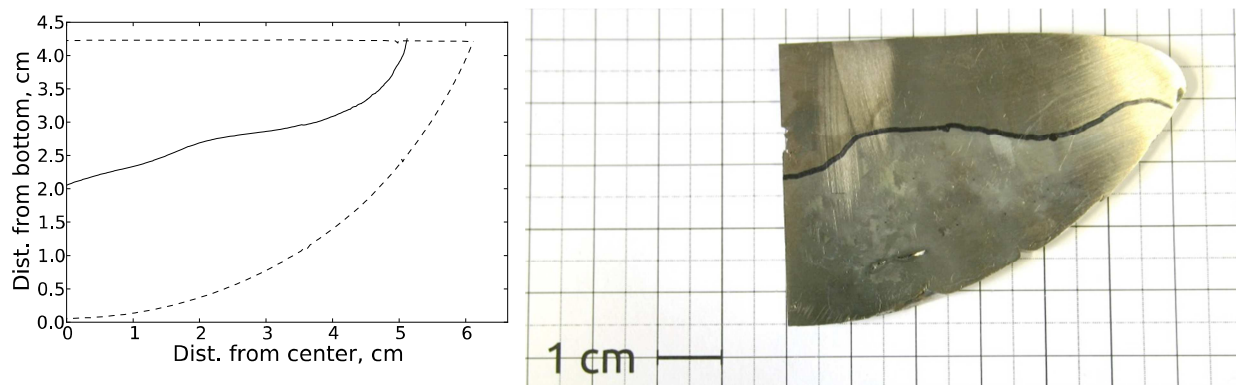


Figure 8. Melt pool profile intersection with plane 3 – (left) computed (right) observed

Qualitatively, the comparison is correct and the calculation reveals the main features of the observed pool: it is significantly larger than the beam pattern and its deepest part is located between the two vertical rectangles of the pattern. These two characteristics of the liquid pool behavior are directly related to the importance of convective heat transfer caused by the Marangoni driven flow. Figs 9 and 10 show the computed velocity field in the N-S center-plane and on top surface.

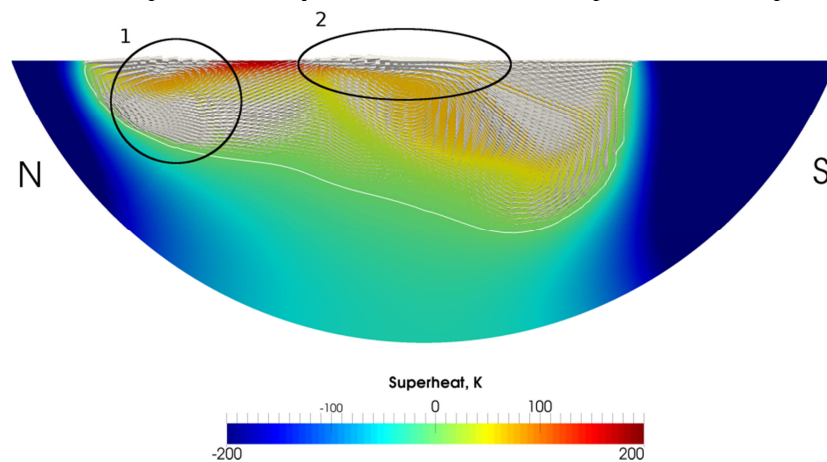


Figure 9. Computed velocity field in the N-S center-plane of the button; 1 – area of strong recirculation in the northern part of the button; 2 – intense flow caused by two jets formed by cumulating Marangoni flow from horizontal and vertical EB pattern rectangles

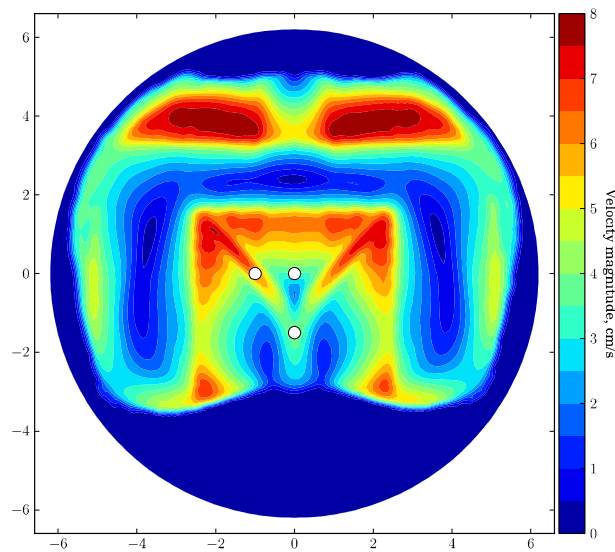


Figure 10. Computed velocity field at the top surface of the button. Rod dipping positions (see next section) are marked with white dots

Indeed, the flow, only weakly turbulent, is fully 3D. It appears to be mainly driven by Marangoni convection: a strong recirculation occurs at the North of the horizontal rectangle, while Marangoni driven jets are created between the two vertical rectangles. The maximum superheat reached at the surface is 210 K, while the maximum velocity is around 8 cm/s. It can be deduced from Figs 6 to 8 that the validity of the prediction is poorer near the edge because of the strong assumption of a flat top surface. A more detailed simulation should account for the deformation of the free surface.

4. Simulation of the influence of rod dipping

Let us recall that, during dissolution experiments, solid material was immersed into the liquid titanium bath [1]. The simple dissolution model requires local values of the velocity, turbulence and temperature in the liquid metal. As it was discussed in the previous section, the data can be obtained from the 3D model described in the paper. However, this approach assumes that presence of the inserted rod itself does not influence significantly the local fluid flow and heat transfer mechanisms.

To check the validity of this assumption, a new set of simulations were performed, where a solid rod was inserted in the steady-state liquid pool formed by the horseshoe electron beam pattern. The solid cylinder had a 4 mm diameter, while the full inserted length was 1.5 cm, which is a bit lower than the maximum pool depth. In order to simplify the calculation and maximize the effect of the presence of the rod, the latter was assumed to remain solid, i.e. no dissolution was accounted for. At the rod-liquid interface, the new version of the model used simple no-slip boundary conditions for fluid flow, wall-functions for turbulence and assumed no heat transfer.

Three dipping positions were simulated, as represented on Fig. 10. The first one is the location of the predicted maximum pool depth, where two jets formed by the Marangoni-driven flow meet, the second one is the geometrical center of the top surface, while the third immersion is localized in one of the Marangoni jets.

The initial liquid pool state corresponds to the steady state computed in the previous section. During the development of the new thermohydrodynamic behavior, first-order discretization schemes were used for the first 5 seconds, after which a switch to second-order schemes was made till the new steady state was reached.

In the case of central dipping position, after an initial perturbation caused by the sudden immersion, a new steady state was reached, which did not differ much from the previous one. Therefore, it can be concluded that the immersion of the rod had only a slight influence on the liquid metal state. In the case of dipping at the location of the deepest pool, the flow field near the free surface was not affected much. However, some perturbations occurred inside the pool. Indeed, more titanium was solidified, so that the solidification front actually reached the tip of the cylinder (no real dissolution of the rod was allowed). In the bulk, the temperature field was not heavily changed.

From the above discussion, it appears that in most cases, results of the 3D model, without actually accounting for the immersion of the refractory sample, can be used in a first approximation as a data set for a simple model of dissolution kinetics. Even though a precise quantitative prediction would require accounting for the effect of the presence of the rod, we must not forget that the dissolution process itself would certainly limit the influence of the sample on the pool behavior.

5. Conclusions

A numerical model of the coupled fluid flow and heat transfer in the liquid bath created by the EB melting of titanium in a hemispherical crucible has been set up. The corresponding 3D solver code was implemented within the OpenFOAM software. Validation was achieved, at least qualitatively, by comparing the predicted 3D pool profile with the observation of an EB melted Ti button in our experimental facility. The model was applied to the calculation of velocities and temperatures during dissolution experiments based on the immersion of refractory samples into the bath. While the 3D model enables us to reach data necessary for dissolution calculations, such an approach does not account for the influence of the presence of a dissolving rod on the behavior of the bath. Therefore, the immersion of a solid cylindrical body which represents a non-dissolving refractory sample was also simulated. Results revealed that the foreign body may slightly disturb the flow in its vicinity. The amount of the disturbance depends on the exact dipping location.

The main features required for improving the model are a better representation of the free surface, assumed here to be flat, and an actual modelling of the dissolution of the immersed rod, not accounted for yet. Anyway, these first results are promising enough so that a 3D modelling of the continuous growth and solidification of a remelted ingot, either an EB or a VAR one, has started at IJL Nancy.

References

- [1] G. Ghazal, P. Chapelle, A. Jardy et al., *ISIJ International* **52** (2012) 1-9.
- [2] T. Quatravaux, S. Ryberon, S. Hans et al., *Journal of Materials Science* **39** (2004) 7183-7191.
- [3] A. Jardy, D. Ablitzer, *Materials Science and Technology* **25** (2009) 163-169.
- [4] V. Weber, A. Jardy, B. Dussoubs et al., *Met. and Mat. Transactions B*, **40** (2009) 271-280.
- [5] M. Revil-Baudard, A. Jardy, H. Combeau et al., *Met. and Mat. Transactions B*, **45** (2014) 51-57.
- [6] S.V. Patankar, D.B. Spalding, *Int. Journal Heat and Mass Transfer* **15** (1972) 1787-1806.
- [7] R.I. Issa, *Solution of the implicit discretized fluid flow equations by operator splitting*, Mechanical Engineering Rep. FS-82-15, Imperial College London, 1982.
- [8] B. van Leer, *Journal of Computational Physics* **14** (1974) 361-370.
- [9] M.R. Hestenes, *Conjugate directions methods in optimization*, Springer, 1980.
- [10] H.A. van der Vorst, *SIAM J. Sci. and Stat. Comput.*, **13** (1992) 631-644.
- [11] H. Jasak, *Error analysis and estimation for the Finite Volume method with applications to fluid flows*, PhD thesis, Imperial College London, 1996.
- [12] OpenFOAM Foundation, <http://openfoam.org>.
- [13] O. Bertrand, B. Binet, H. Combeau et al., *Int. Journal of Thermal Sciences*, **38** (1999) 5-26.
- [14] N. Hannoun, V. Alexiades, T.Z. Mai, *Numerical Heat Transfer B*, **44** (2003) 253-276.
- [15] G. Vidalain, L. Gosselin, M. Lacroix, *Int. Journal Heat and Mass Transfer*, **52** (2009) 1753-1760.